Journal of Applied Polymer Science

Preparation and Properties of Styrene-Butadiene Rubber Nanocomposites Blended with Carbon Black-Graphene Hybrid Filler

Hongmei Zhang, Chunwei Wang, Yong Zhang
State Key Laboratory of Metal Matrix Composites, School of Chemistry and Chemical Engineering, Shanghai Jiao Tong University, Shanghai 200240, People's Republic of China
Correspondence to: H. Zhang (E-mail: hmzhang@sjtu.edu.cn)

ABSTRACT: Graphene has become an attractive reinforcing filler for rubber materials, but its dispersion in rubber is still a big challenge. In this work, a novel carbon black-reduced graphene (CB-RG) hybrid filler was fabricated and blended with styrene-butadiene rubber (SBR) via simple two-roll mill mixing. The prepared CB-RG hybrids had a microstructure with small CB agglomerates adsorbed onto graphene surfaces. CB acted as a barrier preventing the RG sheets from restacking even after drying. Homogeneous dispersion of graphene sheets in SBR matrix was observed by the mechanical mixing method based on the application of the CB-RG hybrid fillers. Dynamic mechanical analysis showed that T*g* of the SBR/CB-RG blend was higher than that of the SBR/CB blend indicating strong interfacial interactions between RG and SBR due to the high surface area of graphene and the π-π interaction between SBR and graphene. The tensile properties of SBR/CB-RG composites improved significantly and the volume resistivity decreased compared with the SBR/CB blends. The thermal stability of SBR composites filled with CB and CB-RG showed slight difference. © 2014 Wiley Periodicals, Inc. J. Appl. Polym. Sci. **2015**, *132*, 41309.

KEYWORDS: composites; elastomers; graphene and fullerenes; mechanical properties; morphology; nanotubes

Received 18 March 2014; accepted 21 July 2014
DOI: 10.1002/app.41309

INTRODUCTION

Addition of fillers, such as silica and carbon black (CB), to rubber produces a well-known reinforcement effect, which can not only reduce the cost, but also significantly improve the mechanical properties.[1] Functional fillers, such as carbon nanotube, graphene, montmorillonoid, and metal nanoparticles, can meanwhile introduce some unique properties to rubber materials and provide a possibility of preparing functional rubber composites.[2–4]

Graphene has drawn a world-wide attention and has been intensively studied and explored in various applications for advanced technologies in recently years due to its fascinating intrinsic properties. With Young's modulus of 1 TPa and ultimate strength of 130 GPa, single-layer graphene is the strongest material ever measured.[5] It has a thermal conductivity of 5000 W/(m* K), which corresponds to the upper bound of the highest values reported for SWCNT bundles.[6] Moreover, single-layer graphene has very high electrical conductivity, up to 6000 S/cm[7] and extremely high surface area (theoretical limit: 2630 m^2/g).[8] These unique properties make graphene to be an attractive reinforcing filler for polymers. As compared to common fillers, such as carbon black and silica, dramatic improvements in mechanical properties of polymer/graphene composites can be achieved at very low filler content and special electrical, thermal and gas barrier properties can be obtained with the incorporation of grapheme.[9–11]

However, the surface energy between graphene and polymer varies considerably, resulting in the lack of thermodynamic driving force for blending. Due to surface characteristic of graphene, it tends to aggregate to reduce the surface energy. Therefore, homogeneous dispersion and efficient interfacial stress transfer become the main challenges for the effective reinforcement. In order to have nano-dispersion of graphene in polymer, the preparation methods, such as in-situ polymerization, solution mixing and coagulating of polymeric composite solution, are normally used, which are inefficient, costly and not conducive to large-scale application.[12–14] Previous researches focused on the surface modification of graphene to enhance the adhesion force between fillers and polymers and to improve the dispersion.[15,16] But in this case, the modifiers sometimes would change the intrinsic properties of graphene. The fabrication of hybrid nanoparticles is a new strategy for nano-dispersion of graphene in rubber matrix. By this method, the strong adsorption between nanoparticles could be weakened, and the respective and synergistic effects of each kind of nanoparticles could be exerted.

Table I. Compositions of SBR/CB-RG(CB) Compounds

Component	SBR/CB-1	SBR/CB-2	SBR/CB-RG-1	SBR/CB-RG-2	SBR/CB-RG-3
SBR	100	100	100	100	100
CB	10	13	-	-	-
CB-RG	-	-	11 (CB:GO=10:1)	12 (CB:GO=10:2)	13 (CB:GO=10:3)
DCP			1		

Previous studies on graphene hybrid nanoparticles mainly concentrated on their preparations and the own performances by far.[17] Reports about applying such hybrid nanoparticles in polymer composites are limited. Das et al.[18] investigated the effect of expanded graphite-multiwalled carbon nanotubes (SWNT) hybrid fillers in styrene-butadiene rubber (SBR) and found that the formation of a mixed filler network showed a synergistic effect on the improvement of electrical as well as various mechanical properties. Yu et al.[19] found that by combining SWNT and graphitic nanoplatelet fillers, a synergistic effect in the thermal conductivity enhancement of epoxy composites was achieved. In Wu's study,[20] a polystyrene composite with graphene–TiO2 nano-sheets exhibited very high permittivity and low dielectric loss. Luo[21] and Wang et al.[22] fabricated a core-shell structured hybrid submicroparticles of graphene oxide-silica (GO-SiO2) and applied this new hybrid filler in maleated polypropylene (PP-g-MA) and poly(vinylidene fluoride) (PVDF) composites. A uniform dispersion of GO-SiO2 hybrids, enhanced interfacial adhesion, and improved mechanical property were evidenced.

Graphene/CB composites have been studied by some researchers for supercapacitor, electrode, and electrocatalyst applications.[23–25] Cai[26] prepared CB/graphene nanoplatelets (GNPs) hybrid fillers filled silicon rubber via one step liquid mixing method. In our study, we prepared dried CB-RG hybrid fillers firstly and then blended them with SBR by commonly used rubber processing method. CB-GO hybrids were first prepared by a simple solution mixing procedure, and then GO was *in situ* reduced by p-phenylene diamine (PPD). It has been proved in Chen's work[27] that PPD acted not only as a reducing agent for GO, but also as a good stabilizer for reduced graphene (RG) because it was positively charged due to the absorption of the oxidation product of PPD (OPPD). The fabricated CB-RG hybrid fillers were then added into SBR by two-roll mill processing. The microstructure and dispersion of CB-RG in SBR were analyzed by scanning electronic microscopy (SEM) and X-ray diffraction (XRD). The mechanical properties, electrical conductivity as well as thermal properties of SBR/CB-RG composites were also investigated. A simple mixing procedure, a uniform dispersion and improved mechanical properties by the application of these CB-RG hybrid fillers in rubber may broaden the application of graphene in the preparation of functionalized and reinforced rubber composites.

EXPERIMENTAL

Materials

SBR was kindly provided by Shenhua Chemical Industrial Co. Ltd., China [1500E, Mooney viscosity ML (1+4) 100°C is 75]. Flake graphite with average particle size of 6 μm was purchased from Qingdao Graphite Co. Ltd. The chemicals include $NaNO_3$, $KMnO_4$, concentrated H_2SO_4, concentrated HCl, dimethyl formamide (DMF), tetrahydrofuran (THF), 30% H_2O_2 aqueous solution and dicumyl peroxide (DCP) were all analytical grade and purchased from Sinopharm Chemical Reagent Co. Ltd., China.

Preparation of CB-RG Hybrid Fillers

GO was prepared from natural graphite by the modified Hummers' method.[12,28] Briefly, flake graphite (5 g) and $NaNO_3$ (3 g) with concentrated H_2SO_4 (120 mL, 98%) were put into a flask and under stirring in an ice water bath. $KMnO_4$ (22.5 g) was slowly added to the above mixture and followed by continuously stirring at 23°C for 2 h. Then H_2SO_4 aqueous solution (700 mL, 5 wt %) was slowly added under stirring, and the temperature was kept at 98°C. When the temperature was decreased to 60°C, H_2O_2 aqueous solution (15 mL, 30 wt %) was added. The product was washed with HCl solution (5 wt %) and distilled water several times and freeze-dried.

CB-RG hybrid fillers were fabricated by *in situ* reduction of GO by PPD in CB/GO suspension. 100mg GO was dispersed in water (100 mL) in an ultrasonic bath for 1 h at 23°C to yield a stable solution. After that, 1.0 g of CB was added into GO solution followed by further ultrasonication for 1 h to form uniform suspension of CB/GO mixture. Meanwhile, PPD (1.0 g) was dissolved in ethanol (50 mL) at room temperature and added into the CB/GO mixture. The CB/GO suspension with PPD incorporated was stirred and refluxed in a water bath at 90°C for 24 h. The obtained CB-RG hybrids were filtrated and washed with ethanol several times to remove unreacted PPD and its oxydate, and then dried in vacuum oven. The dried CB-RG hybrids were grounded into powder before use. CB-RG hybrid fillers with different compositions were prepared by changing the ratio between CB and GO as 10:1, 10:2, and 10:3.

Preparation of SBR/CB-RG Composites

SBR, CB or CB-RG hybrids and dicumyl peroxide (DCP) were mixed on a two-roll mill at room temperature to prepare SBR/CB-RG compounds. The resulting compounds were then cured at 170°C for 20 min under a pressure of 15 MPa. The compositions of the SBR/CB-RG(CB) compounds are given in Table I.

Characterization

Atomic force microscopy (AFM) images of GO were taken in a tapping mode by performing on a Nano Scope III A (Digital Instrument, USA). The GO/DMF solution was spin-coated onto freshly cleaved mica substrates at 2000 rpm and dried under vacuum at 80°C for AFM characterization. SEM images of CB,

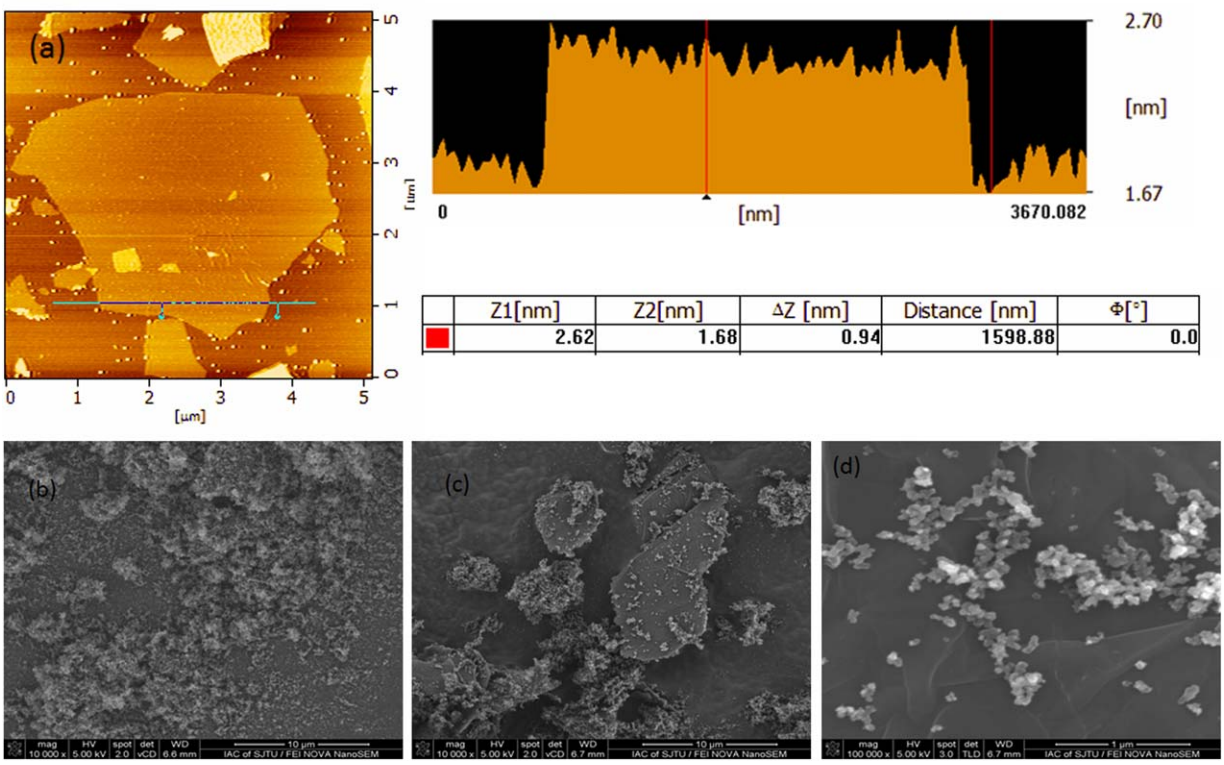

Figure 1. (a) A typical tapping mode AFM image of G-O nanosheet; (b) SEM image of CB; (c) SEM image of CB-RG (10,000×); (d) SEM image of CB-RG (100,000×). [Color figure can be viewed in the online issue, which is available at wileyonlinelibrary.com.]

CB-RG and SBR/CB-RG(CB) composites were obtained on a Hitachi S-2150 field-emission SEM system. SBR/CB-RG(CB) samples were fractured in liquid nitrogen and the fracture surfaces were observed. X-ray diffraction (XRD) spectra were recorded by D/max-2200/PC (Japan Rigaku Corp.) using Cu Kα radiation. Tensile tests were performed on a SANS instrument at room temperature at a crosshead speed of 500 mm/min. The dumbbell shape samples were 75 mm in length, 4 mm in width, and 1 mm in thickness. Volume resistance test was carried out under the voltage of 500V. The diameter of samples is 8 cm and the area of samples is 50.27 cm^2. DMA spectra were recorded for rectangular specimens (40 × 5 × 1 mm^3) in tension mode as a function of temperature (from −70 to 100°C) at a frequency of 10 Hz with a dynamic mechanical analyzer (Viscoelasticity Analyzer VR7120, Japan). Tests were run at a constant strain (0.25%) through the heating scan of the specimens in a stepwise manner (stepping by 3°C). TGA was tested in nitrogen with a Perkin Elmer TGA 2050 instrument at a heating 70 rate of 20°C/min over a temperature range of 20–700°C.

RESULTS AND DISCUSSION

Figure 1(a) shows the typical AFM morphology of GO nanosheets prepared by Hummers methods in this study. A thin and large single-layer GO sheet with about 300 nm in both width and length was observed. Analysis of AFM images revealed that most GO sheets were about 0.9 nm in thickness, which indicates that graphite was fully exfoliated into monolayers.[29] The prepared GO can be homogenously dispersed in water after mild sonication. The SEM morphology of dried CB and CB-RG fillers are shown in Figure 1(b,c). Mono-layer or few-layer RG sheets were observed with small CB agglomerates adsorbed onto their surface. After further magnification, wrinkles of graphene can be observed in Figure 1(d) for CB-RG fillers. It is known that restacking of graphene flat sheets, especially after chemical reduction, is a big challenge for the effective application. In previous studies, restacking was prevented by either use of surfactants that can stabilize the reduced particle suspensions or blending with polymers prior to the chemical reduction. In our study, on one hand, the reducing agent PPD might act as a good stabilizer for RG, and on the other hand, CB particles deposited on the planes of graphene also prevented the RG sheets from restacking even after drying.

The dried and grounded CB-RG hybrid fillers were then compounded with SBR on a two-roll mill. The dispersion conditions of CB and CB-RG in SBR matrix were observed by SEM and TEM as shown in Figure 2. The small white spots in Figure 2(a) can be attributed to CB fillers. For the composites filled with CB-RG, besides CB fillers, some RG sheets pulled out of the SBR matrix were also observed from the cross-section of the composite as pointed by the arrows in Figure 2(b) and no obvious RG aggregates were observed. Figure 2(c,d) by TEM measurements further confirmed the homogenous dispersion of graphene sheets in the rubber matrix. This result indicates that the homogeneous dispersion of graphene sheets can be obtained by mechanical mixing method based on the application of hybrid CB-RG fillers. Compared to solution mixing method on

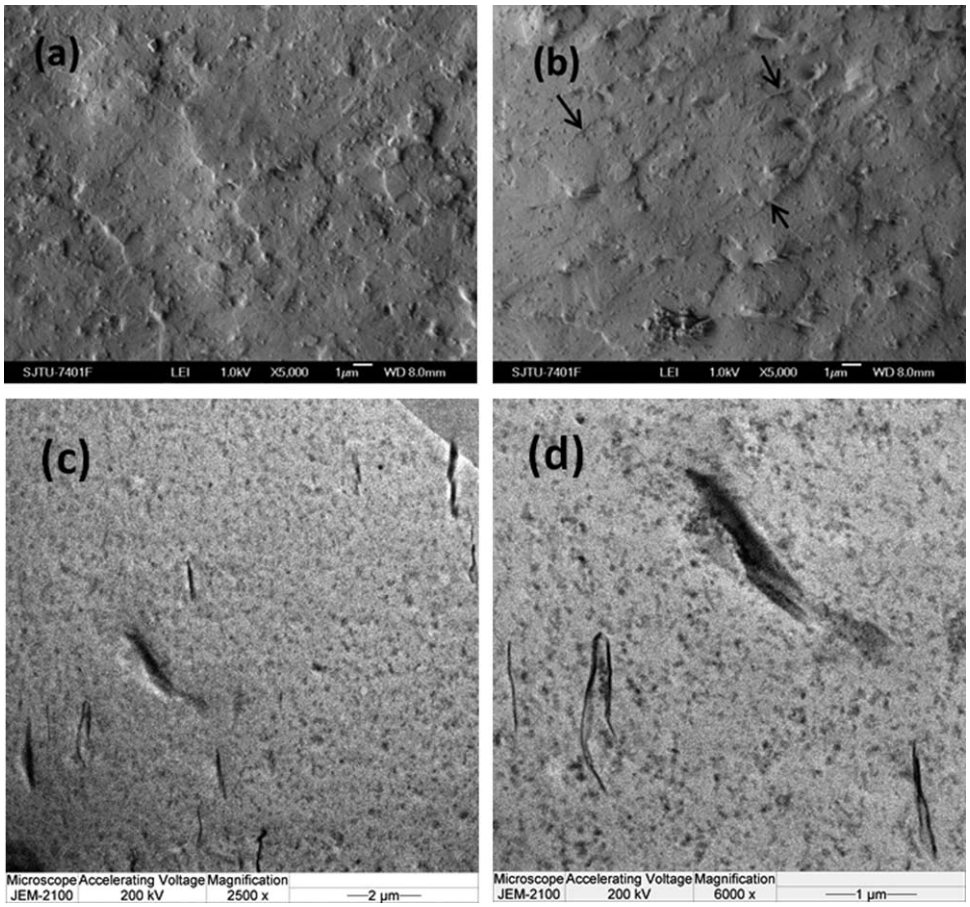

Figure 2. (a) SEM cross-sectional images of SBR/CB; (b) SEM cross-sectional images of SBR/CB-RG composites; (c) and (d) TEM images of SBR/CB-RG composites.

preparing polymer/graphene composites, the mechanical mixing method is more simple, environmental friendly and economic beneficial. Moreover, a certain orientation of graphene sheets was observed due to the two-roll mill processing method, which is difficult to be achieved by solution mixing method as well.

XRD is a powerful method for the study of nanomaterials and the dispersion of nanofillers in polymer matrix.[30,31] Figure 3(a) shows the XRD patterns of graphite, GO, CB, and CB-RG hybrids. The XRD pattern of graphite has a diffraction peak appeared at $2\theta = 26.5°$, indicating the interlayer spacing between graphite layers was 0.35 nm according to the Bragg equation. After being oxidized, the diffraction peak shifted to 11.0°, which means that the interlayer spacing between layers was expanded to 0.80 nm for GO. A broad diffraction peak was observed for CB, indicating its noncrystalline structure. For the hybrid CB-RG fillers, when the ratio between CB and RG was 10 to 1, only a broad diffraction peak of CB was observed, which means that RG sheets have been exfoliated into monolayers or few layers with CB acting as a barrier and preventing the RG sheets from restacking. With higher RG loading, a small diffraction peak at 7.4° appeared as observed at the curves of CB-RG (10:2) and CB-RG (10:3), corresponding to a interlayer spacing of 1.2 nm, which was larger than that of GO. When the RG loading increased, some part of the graphene layers did not separate completely, but still some CB particles might be inserted into the RG layers, which enlarged the interlayer spacing.

The XRD patterns of SBR/CB and SBR/CB-RG composites are shown in Figure 3(b). A broad diffraction peak at around 20° can be observed for all the blends. The SBR blend filled with CB-RG (10:1) showed the same behavior as filled with CB, which again indicated the fully exfoliation of RG sheets and good dispersion of RG in polymer matrix. When the ratio between CB and RG changed to 10:2 and 10:3, a small peak at around 7.6° appeared again, which was consistent with the results for CB-RG fillers in Figure 3(a). Therefore, when the RG amount increased, some stacked RG with small amount of CB in between existed in the SBR matrix.

The dynamic mechanical properties of SBR/CB and SBR/CB-RG blends are shown in Figure 4. For the SBR/CB blends, the T*g* shifted slightly to higher temperature when the CB amount increased from 10 phr to 13 phr because that the chain mobility was restrained to higher extent with more CB added. For the CB-RG filled blends, the DMA curve of the blend with 1 phr RG was almost coincident with that of SBR/CB blend filled with13 phr CB. By increasing the RG loading, the T*g* shifted to higher temperature furthermore. Comparing the two blends

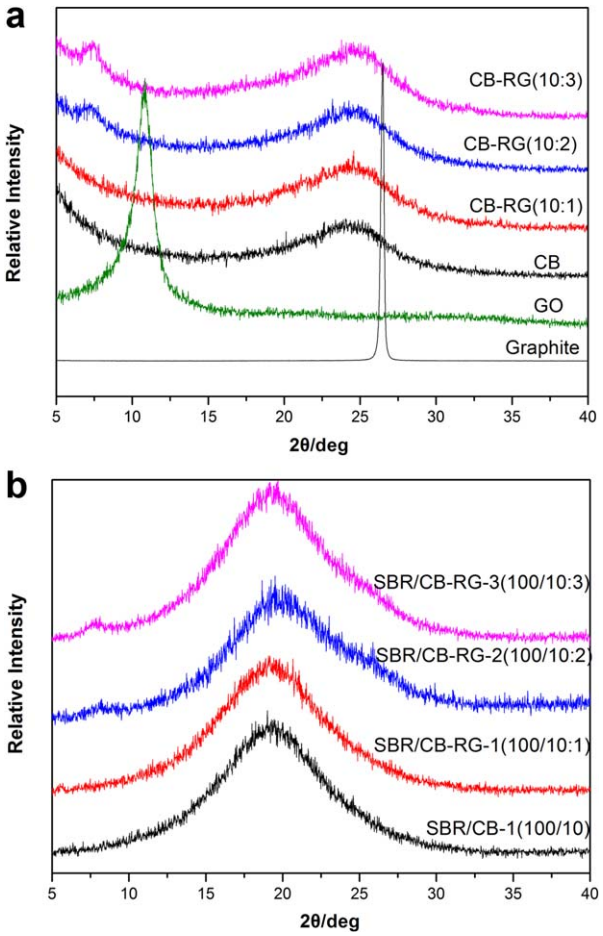

Figure 3. XRD patterns of (a) graphite, GO, CB, and CB-RG hybrids; (b) SBR/CB and SBR/CB-RG composites. [Color figure can be viewed in the online issue, which is available at wileyonlinelibrary.com.]

with the same total filler loading, SBR/CB-RG (100/10:3) had higher T*g* than that of SBR/CB (100/13), which means that RG restrained the chain mobility of SBR to higher extent under low-strain tension mode. This might be due to the extremely high surface area of graphene and the π-π interaction between the π-conjugated network on the surface of RG and the aromatic groups of SBR. Then efficient reinforcement of graphene on SBR was expected.

The tensile curves of SBR/CB and SBR/CB-RG composites are shown in Figure 5 and the data are summarized in Table II. The SBR/CB blends with 10 phr and 13 phr CB were prepared for comparison considering the using range of the total amount of CB and RG for the SBR/CB-RG blends. For the SBR/CB blends, limited improvements on the tensile properties were observed when the CB amount increased from 10 phr to 13 phr. When CB-RG hybrid fillers were applied, significant improvements were found. The moduli at 200% elongation (M200) of the SBR/CB-RG blends were higher than those of the SBR/CB blends at no expense of elongation. The elongation at break even increased from 260% to 300% when 1 phr of RG was applied compared to the SBR/CB blend filled with 10 phr CB. The tensile strength of the blends was enhanced from 3.5 to 4.9

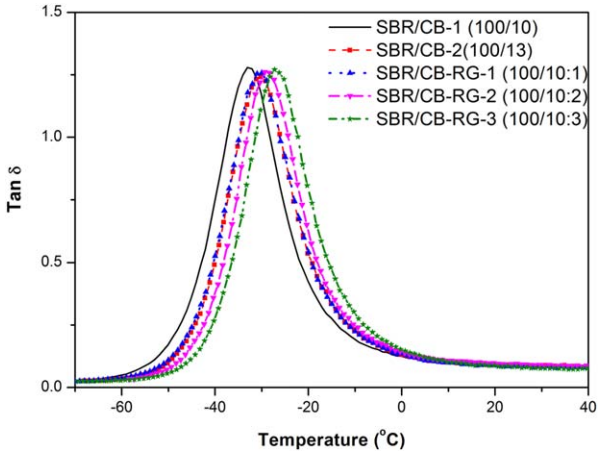

Figure 4. DMA curves of SBR/CB and SBR/CB-RG composites with different filler loadings. [Color figure can be viewed in the online issue, which is available at wileyonlinelibrary.com.]

MPa, increased as much as 40% after addition of 1 phr RG. The enhancement of the tensile properties after the application of CB-RG hybrid filler compared to single CB filler can be attributed to the better reinforcement effect of RG on SBR matrix. When the amount of RG increased to 2 and 3 phr, M200 increased furthermore. But the improvements on tensile strength and elongation at break were not pronounced. Therefore, no more enhancements on tensile strength and elongation at break could be obtained with even higher RG content. On one hand, more graphene incorporated only resulted in higher modulus but lower tensile strength and elongation at break after the optimum filler loading. On the other hand, as has been proven by the XRD measurements in previous discussion, when the RG amount increased and the ratio between CB and RG changed to 10:2 and 10:3, some stacked RG still existed in SBR matrix and the RG sheets were not dispersed in fully exfoliation status, which might impair the reinforcement effect of graphene for SBR to some extent.

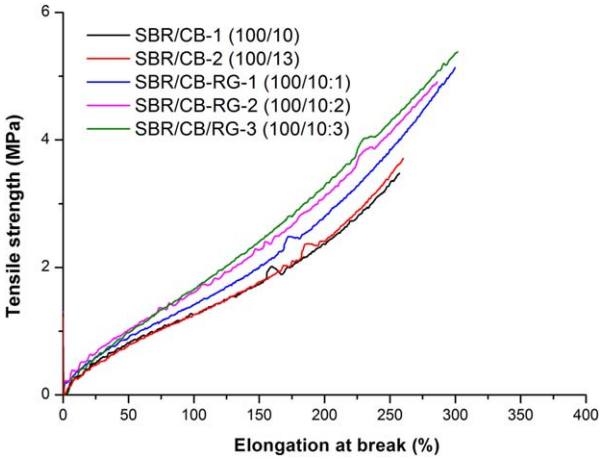

Figure 5. Representative stress–strain behavior for SBR/CB and SBR/CB-RG composites with different filler loadings. [Color figure can be viewed in the online issue, which is available at wileyonlinelibrary.com.]

Table II. Mechanical Properties and Volume Resistivity of SBR/CB-RG(CB) Composites

Rubber	CB-RG(CB) contents (CB/GO)	Tensile strength (MPa)	Elongation at break (%)	M200 (MPa)	Volume resistivity (Ω cm)
SBR (100 phr)	10 phr/0 phr	3.5 ± 0.2	260 ± 10	2.3 ± 0.1	2.08×10^{13}
	13 phr/0 phr	3.8 ± 0.4	270 ± 20	2.4 ± 0.2	2.26×10^{13}
	10 phr/1 phr	4.9 ± 0.3	300 ± 20	2.8 ± 0.2	3.22×10^{12}
	10 phr/2 phr	4.8 ± 0.3	280 ± 20	3.1 ± 0.2	1.30×10^{12}
	10 phr/3 phr	5.3 ± 0.4	300 ± 30	3.3 ± 0.3	9.50×10^{11}

Volume resistivity tests were done to check the electrical conductivity of the blends and the volume resistivity values of the SBR/CB and SBR/CB-RG blends are listed in Table II. The volume resistivity of the SBR/CB blends filled with 10 and 13 phr CB was more or less the same. After the application of CB-RG hybrid fillers, the volume resistivity decreased by one order of magnitude as compared to the single CB filler. With increasing amount of RG, the volume resistivity decreased slightly. Therefore, with the same filler loading, CB-RG hybrid filler could introduce higher electrical conductivity to SBR composites than single CB filler due to the intrinsic high electrical conductivity of graphene.

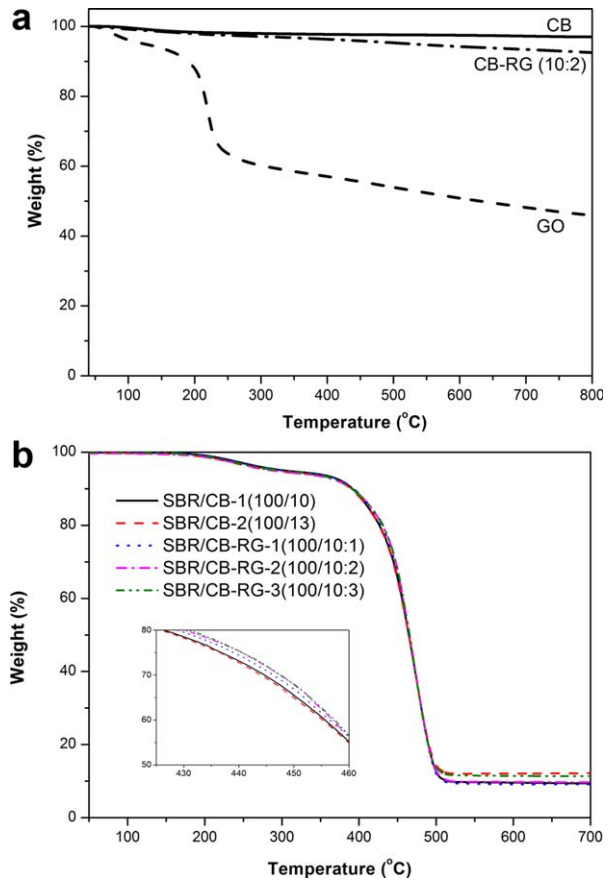

Figure 6. TGA curves of (a) CB, GO, and CB-RG hybrid filler; (b) SBR/CB and SBR/CB-RG composites. [Color figure can be viewed in the online issue, which is available at wileyonlinelibrary.com.]

Besides the tensile and dynamic mechanical properties, we further investigated the thermal properties of CB-RG fillers and SBR composites by TGA measurements. Weight loss curves of CB, GO and CB-RG (10:2) fillers are shown in Figure 6(a). In nitrogen atmosphere, the CB curve showed a little weight loss about 3.0 wt % till 800°C. The decomposition of GO took place in two steps. In the temperature range less than 150°C, the weight loss of GO was mainly attributed to the evaporation of water absorbed on the graphene sheets. The pyrolysis of labile oxygen-containing groups, such as –COOH, -OH etc., resulted in the weight decrease of GO from 200 to 300°C. After that the weight loss got slower and the char yield of GO was 46.0 wt % till 800°C. The weight loss of CB-RG in the whole temperature range was slow and the final char yield was about 92.5 wt %. According to the char yield of pure CB and pure GO, the calculated char yield of a simple CB/GO composite at a ratio of 10 to 2 was 88.5 wt % which was less than the char yield of CB-RG at the same ratio. This indicated that after the reduction of GO by PPD, the amount of oxygen-containing groups reduced and the thermal stability of CB-RG hybrid filler increased.

The thermal stability of SBR composites filled with CB and CB-RG showed no significant difference. The weight loss curves of SBR/CB-RG composites slightly shifted towards higher temperature in the range from 400 to 460°C compared to SBR/CB composites. High aspect ratio of monodispersed graphene layers might act as barrier and inhibit the emission of small gaseous molecules, resulting in better thermal stability. But due to the limited amount of graphene in our composites, the effect was not obvious.

CONCLUSIONS

CB-RG hybrid fillers were prepared by *in situ* reduction of GO by PPD in CB/GO water suspension. SEM and XRD measurements demonstrated that RG sheets have been exfoliated into monolayers or few layers with CB acting as a barrier preventing the RG sheets from restacking after drying. SBR/CB-RG composites were prepared via two-roll mill mixing. The graphene sheets were dispersed homogenously in SBR matrix as observed by SEM and TEM. The increase of T*g* after the incorporation of CB-RG indicated strong interfacial interactions between RG and SBR due to the extremely high surface area of graphene and the π-π interaction. The tensile properties of the SBR/CB-RG composites were much better compared with the SBR/CB blends. The volume resistivity decreased after the application of CB-RG

hybrid fillers compared to single CB filler due to the intrinsic high electrical conductivity of graphene. TGA results indicated that after the reduction of GO by PPD, the amount of oxygen-containing groups reduced. The thermal stability of SBR composites filled with CB and CB-RG showed no significant difference.

ACKNOWLEDGMENTS

Financial supports from the National Natural Science Foundation of China (Project numbers 51303103).

REFERENCES

1. Guido, R. *Macromol. Theory Simul.* **2003**, *12*, 17.
2. Göske, J.; Kachler, W.; Seeger, C.; Risch, A. *Kautsch Gummi Kunstst.* **2009**, *62*, 430.
3. Atieh, M. A. *J. Thermoplast. Compos.* **2011**, *24*, 613.
4. Al-Juaid, S. S.; El-Mossalamy, E. H.; Arafa, H. M.; Al-Ghamdi, A. A.; Abdel Daiem, A. M.; El-Tantawy, F. *J. Appl. Polym. Sci.* **2011**, *121*, 3604.
5. Lee, C.; Wei, X.; Kysar, J. W.; Hone, J. *Science* **2008**, *321*, 385.
6. Balandin, A. A.; Ghosh, S.; Bao, W.; Calizo, I.; Teweldebrhan, D.; Miao, F.; Lau, C. N. *Nano Lett.* **2008**, *8*, 902.
7. Du, X.; Skachko, I.; Barker, A.; Andrei, E. Y. *Nat. Nanotechnol.* **2008**, *3*, 491.
8. Stoller, M. D.; Park, S.; Zhu, Y.; An, J.; Ruoff, R. S. *Nano Lett.* **2008**, *8*, 3498.
9. Ramanathan, T.; Abdala, A. A.; Stankovich, S.; Dikin, D. A.; Herrera-Alonso, M.; Piner, R. D.; Adamson, D. H.; Schniepp, H. C.; Chen, X.; Ruoff, R. S.; Nguyen, S. T.; Aksay, I. A.; Prud'Homme, R. K.; Brinson, L. C. *Nat. Nanotechnol.* **2008**, *3*, 327.
10. Kim, H.; Miura, Y.; Macosko, C. W. *Chem. Mater.* **2010**, *22*, 3441.
11. Liang, J.; Wang, Y.; Huang, Y.; Ma, Y.; Liu, Z.; Cai, J.; Zhang, C.; Gao, H.; Chen, Y. *Carbon* **2009**, *47*, 922.
12. Bai, X.; Wan, C.; Zhang, Y.; Zhai, Y. *Carbon* **2011**, *49*, 1608.
13. Kim, J.; Hong, S.; Park, D.; Shim, S. *Macromol. Res.* **2010**, *18*, 558.
14. Lee, Y. R.; Raghu, A. V.; Jeong, H. M.; Kim, B. K. *Macromol. Chem. Phys.* **2009**, *210*, 1247.
15. Wu, J.; Huang, G.; Li, H.; Wu, S.; Liu, Y.; Zheng, J. *Polymer* **2013**, *54*, 1930.
16. Zheng, J.; Di, C.; Liu, Y.; Liu, H.; Guo, Y.; Du, C.; Wu, T.; Yu, G.; Zhu, D. *Chem Commun.* **2010**, *46*, 5728.
17. Bai, S.; Shen, X. *RSC Adv.* **2012**, *2*, 64.
18. Das, A.; Kasaliwal, G. R.; Jurk, R.; Boldt, R.; Fischer, D.; Stöckelhuber, K. W.; Heinrich, G. *Compos. Sci. Technol.* **2012**, *72*, 1961.
19. Yu, A.; Ramesh, P.; Sun, X.; Vekyarova, E.; Itkis, M. E.; Haddon, R. C. *Adv. Mater.* **2008**, *20*, 4740.
20. Wu, C.; Huang, X.; Xie, L.; Wu, X.; Yu, J.; Jiang, P. *J. Mater. Chem.* **2011**, *21*, 17729.
21. Luo, F.; Chen, L.; Ning, N.; Wang, K.; Chen, F.; Fu, Q. *J. Appl. Polym. Sci.* **2012**, *125*, 348.
22. Wang, J. C.; Chen, P.; Chen, L.; Wang, K.; Deng, H.; Chen, F.; Zhang, Q.; Fu, Q. *Exp. Polym. Lett.* **2012**, *6*, 299.
23. Liu, Q.; Zhang, H.; Zhong, H.; Zhang, S.; Chen, S. *Electrochim. Acta* **2012**, *81*, 313.
24. Miao, X.; Pan, K.; Pan, Q.; Zhou, W.; Wang, L.; Liao, Y.; Tian, G.; Wang, G. *Electrochim. Acta* **2013**, *96*, 155.
25. Yan, J.; Wei, T.; Shao, B.; Ma, F.; Fan, Z.; Zhang, M.; Zheng, C.; Shang, Y.; Qian, W.; Wei, F. *Carbon* **2010**, *48*, 1731.
26. Cai, W.; Huang, Y.; Wang, D.; Liu, C.; Zhang, Y. *J Appl Polym Sci* **2014**, *131*, DOI: 10.1002/APP.39778.
27. Chen, Y.; Zhang, X.; Yu, P.; Ma, Y. *Chem. Commun.* **2009**, *30*, 4527.
28. Hummers, W. S.; Offeman, R. E. *J. Am. Chem. Soc.* **1958**, *80*, 1339.
29. Park, S.; Ruoff, R. S. *Nat. Nanotechnol.* **2009**, *4*, 217.
30. Liang, J.; Huang, Y.; Zhang, L.; Wang, Y.; Ma, Y.; Guo, T.; Chen, Y. *Adv. Funct. Mater.* **2009**, *19*, 2297.
31. Yang, X.; Tu, Y.; Li, L.; Shang, S.; Tao, X. *ACS Appl. Mater. Interfaces* **2010**, *2*, 1707.